WATER RESOURCES RESEARCH, VOL. 44, W09407, doi:10.1029/2007WR006035, 2008

Eawag 05291

Traveltime-based descriptions of transport and mixing in heterogeneous domains

Jian Luo[1] and Olaf A. Cirpka[2]

Received 13 March 2007; revised 6 May 2008; accepted 4 June 2008; published 4 September 2008.

[1] Modeling mixing-controlled reactive transport using traditional spatial discretization of the domain requires identifying the spatial distributions of hydraulic and reactive parameters including mixing-related quantities such as dispersivities and kinetic mass transfer coefficients. In most applications, breakthrough curves (BTCs) of conservative and reactive compounds are measured at only a few locations and spatially explicit models are calibrated by matching these BTCs. A common difficulty in such applications is that the individual BTCs differ too strongly to justify the assumption of spatial homogeneity, whereas the number of observation points is too small to identify the spatial distribution of the decisive parameters. The key objective of the current study is to characterize physical transport by the analysis of conservative tracer BTCs and predict the macroscopic BTCs of compounds that react upon mixing from the interpretation of conservative tracer BTCs and reactive parameters determined in the laboratory. We do this in the framework of traveltime-based transport models which do not require spatially explicit, costly aquifer characterization. By considering BTCs of a conservative tracer measured on different scales, one can distinguish between mixing, which is a prerequisite for reactions, and spreading, which per se does not foster reactions. In the traveltime-based framework, the BTC of a solute crossing an observation plane, or ending in a well, is interpreted as the weighted average of concentrations in an ensemble of non-interacting streamtubes, each of which is characterized by a distinct traveltime value. Mixing is described by longitudinal dispersion and/or kinetic mass transfer along individual streamtubes, whereas spreading is characterized by the distribution of traveltimes, which also determines the weights associated with each stream tube. Key issues in using the traveltime-based framework include the description of mixing mechanisms and the estimation of the traveltime distribution. In this work, we account for both apparent longitudinal dispersion and kinetic mass transfer as mixing mechanisms, thus generalizing the stochastic-convective model with or without inter-phase mass transfer and the advective-dispersive streamtube model. We present a nonparametric approach of determining the traveltime distribution, given a BTC integrated over an observation plane and estimated mixing parameters. The latter approach is superior to fitting parametric models in cases wherein the true traveltime distribution exhibits multiple peaks or long tails. It is demonstrated that there is freedom for the combinations of mixing parameters and traveltime distributions to fit conservative BTCs and describe the tailing. A reactive transport case of a dual Michaelis-Menten problem demonstrates that the reactive mixing introduced by local dispersion and mass transfer may be described by apparent mean mass transfer with coefficients evaluated by local BTCs.

Citation: Luo, J., and O. A. Cirpka (2008), Traveltime based descriptions of transport and mixing in heterogeneous domains, *Water Resour. Res.*, *44*, W09407, doi:10.1029/2007WR006035.

1. Introduction

[2] Dilution and mixing in subsurface media have been recognized as a critical issue for successful remediation of contaminated groundwater and soil [*Lee et al.*, 1988; *Molz and Widdowson*, 1988; *Sturman et al.*, 1995; *Cirpka et al.*, 1999b]. Mechanisms that may create mixing include the following: (1) local dispersion, (2) kinetic mass transfer between mobile and immobile phases, (3) chromatographic effects, and (4) hydrodynamic instability [*Oya and Valocchi*, 1998; *Weeks and Sposito*, 1998; *Cirpka et al.*, 1999b; *Cirpka*, 2005]. By contrast, macrodispersion, mainly describing the spreading of a plume at field scales, cannot be used as a measure of dilution and mixing [*Kitanidis*, 1994]. Modeling dilution and mixing in heterogeneous media

[1]School of Civil and Environmental Engineering, Georgia Institute of Technology, Atlanta, Georgia, USA.
[2]Swiss Federal Institute of Aquatic Science and Technology (Eawag), Dübendorf, Switzerland.

0043-1397/08/2007WR006035$09.00

using traditional spatial discretization of the domain requires identifying the spatial distribution of hydraulic conductivity and mixing-related transport parameters such as local dispersivities and kinetic mass transfer coefficients. A particular challenge lies in predicting mixing-controlled reactive transport in heterogeneous domains. If mean concentrations of reactive species are predicted by solving macroscopic advective-dispersive-reactive transport, calibrated by fitting mean conservative concentrations, the degree of mixing and related reaction rates will be overestimated [*Molz and Widdowson*, 1988; *Semprini and McCarty*, 1991; *Ginn et al.*, 1995; *Sturman et al.*, 1995; *Miralles Wilhelm et al.*, 1997; *Cirpka et al.*, 1999b]. Bimolecular reactive transport experiments, conducted by *Raje and Kapoor* [2000] and *Gramling et al.* [2002], demonstrated that even in nearly homogeneous porous media the reaction rates were overestimated by mean advective-dispersive-reactive transport models with transport parameters fitted from average concentration breakthrough curves (BTCs) of conservative tracers.

[3] As an alternative to spatial advection-dispersion equations, characterization of mixing in terms of traveltimes may allow transport descriptions independent of specific mixing mechanisms. As a form of black-box analysis, stochastic-convective models using traveltime distributions are well suited to simulate BTCs at observation points and in control planes. The main advantage of simulating transport in the traveltime domain is that transport becomes one-dimensional with a uniform "velocity" whereas traditional spatial models describe transport in a multidimensional domain with potentially highly variable velocity [*Simmons et al.*, 1995; *Crane and Blunt*, 1999; *Cirpka and Kitanidis*, 2001]. Traveltime-based models are capable of simulating transport in highly nonuniform flow fields or highly heterogeneous media, where highly spatially variable velocity fields can cause anomalous transport and highly asymmetric BTCs, which may not be described well by traditional advective-dispersive transport with uniform velocity and dispersion coefficients [e.g., *Selroos and Cvetkovic*, 1992; *Berkowitz and Scher*, 1997, 1998; *Berkowitz et al.*, 2000; *Di Donato et al.*, 2003; *Di Donato and Blunt*, 2004; *Berkowitz et al.*, 2006; *Fiori et al.*, 2006]. Finally, the traveltime distributions needed for the approach may be conveniently evaluated through conservative-tracer tests; the aquifer heterogeneity does not need to be characterized in a spatially explicit form [*Simmons*, 1982; *Simmons et al.*, 1995]. This advantage is particularly useful for a long-term groundwater remediation project because it is questionable that initial spatial characterizations are applicable in a long-term groundwater remediation project because many factors may alter subsurface conditions, such as biomass accumulation, gas production, and solids precipitation, etc. [*Luo et al.*, 2007]. By contrast, traveltime distributions, which can be conveniently updated by tracer tests, are more flexible to simulate such a long-term reactive system.

[4] In applications to mixing-controlled reactive transport, the traveltime formulation can be modified to distinguish between mixing on the scale of reaction, and spreading, which is a strictly macroscopic phenomenon. In this methodology, longitudinal mixing is described by mixing mechanisms associated with traveltimes, and spreading is expressed by the distribution of advective traveltimes. In the advective-dispersive streamtube approach [*Cirpka and Kitanidis*, 2000a, 2000b], local BTCs, obtained from point-like measurements of conservative compounds, are used to infer apparent, mixing-relevant longitudinal dispersivities. *Cirpka and Kitanidis* [2000b] represented heterogeneous advection by a parametric traveltime distribution, which they estimated from the local mixing parameters and from spatially integrated BTCs, measured at outflow boundaries and/or control planes. *Rubin et al.* [1997] and *Rubin and Ezzedine* [1997] suggested to parameterize transport by a stochastic-convective model with mass transfer, estimating traveltime distributions from local measurements, especially from concentration peaks of local BTCs, and accounting for mixing by kinetic mass transfer. *Robinson and Viswanathan* [2003] used the maximum mixing state for describing reactive transport, which stemmed from the micro-mixing theory developed in chemical engineering [*Nauman and Buffham*, 1983]. However, the maximum mixing state cannot be related to specific physical mixing mechanisms.

[5] All traveltime-based models mentioned above are associated with two key issues: the conceptualization and quantification of effective mixing mechanisms and the estimation of the traveltime distribution. The original stochastic-convective model (or complete segregation in chemical engineering) neglects local mixing altogether. Thus it cannot be used to simulate transport of compounds that react upon mixing. The advective-dispersive streamtube model uses apparent local longitudinal dispersion to characterize mixing and completely neglects mass transfer mechanisms. When the traveltime distribution is estimated by a standard two-parametric model, as done by *Cirpka and Kitanidis* [2000a, 2000b], it cannot be applied to systems where the true traveltime distribution is multimodal, or exhibits other non-traditional features such as long tails. In contrast to the advective-dispersive streamtube model, the stochastic-convective model with mass transfer accounts for exchange with an immobile phase, which generates local mixing, but completely neglects local dispersion. If in this approach the mass transfer model is used to describe mixing effects resulting from various mixing mechanisms, it can no more reflect the actual inter-phase mass transfer behavior. Thus mass transfer information inferred from core samples may not be used. Furthermore, it is challenging to estimate the traveltime distribution based on local BTCs alone because characterizing multimodal, asymmetric traveltime distributions based on point estimates requires an extremely large number of measurement points.

[6] In the present study, we present a general formulation of traveltime-based description of transport, which extends the advective-dispersive streamtube model by incorporating kinetic mass transfer between mobile and immobile phases. In addition, and more importantly, we focus on the two key issues associated with the traveltime framework, i.e., identifying appropriate mixing parameters and estimating traveltime distributions from spatially integrated BTCs. We seek to investigate the questions: (1) how should we choose effective mixing parameters and estimate traveltime distributions and (2) which traveltime model predicts reactive transport best?

[7] The present study is different from the studies mentioned above in the following points:

[8] 1. The procedure proposed here to set up a traveltime-based model is opposite to the models proposed by *Rubin et al.* [1997], in which traveltime distributions were determined followed by mass transfer parameters. By contrast, we prefer to estimate mixing parameters first and then traveltime distributions.

[9] 2. Transport and mixing processes considered include local dispersion and kinetic mass transfer in heterogeneous media.

[10] 3. The model setup procedure allows applying nonparametric methods of estimating traveltime distributions which enables identifying non-traditional features of the traveltime distributions, such as multiple peaks, which would remain undiscovered when a parametric model of the distribution was used.

[11] 4. We compare the performances of different traveltime-based models in simulating reactive transport because flexibilities in combining mixing descriptions and traveltime distributions may generate similar results for conservative tracer data, but different results for reactive systems. We restrict our analysis to problems with uniform mixing parameters, that is, kinetic mass transfer and local dispersivity are assumed uniform even though the velocity field may be heterogeneous.

[12] The article is organized as follows: section 2 summarizes the traveltime-based models mentioned above. Section 3 recapitulates the governing equations of solute transport undergoing kinetic mass transfer using spatial coordinates and discusses the effects of various processes on mixing in heterogeneous media. Section 4 presents the traveltime-based descriptions of transport used in this study. Section 5 outlines the approaches to estimate traveltime distributions. Section 6 presents numerical test cases, in which two-dimensional transport of a compound undergoing kinetic mass transfer in a heterogeneous domain is used to simulate the presumably true concentration distribution, and the various traveltime-based models are subsequently applied to analyze BTCs generated by the spatially explicit model, and to simulate reactive transport of a kinetic dual Michaelis-Menten problem. Finally, in section 7 we draw conclusions.

2. Background

[13] The stochastic-convective representation is the simplest approach for transport simulation using traveltime distributions. Solutes are assumed to be advected through discrete, non-interacting streamtubes [*van der Zee and van Riemsdijk*, 1987; *Shapiro and Cvetkovic*, 1988; *Simmons et al.*, 1995]. Then, the BTC of a conservative compound corresponding to a unit impulse injection is identical to the probability density function (*pdf*) of traveltime. Advective-reactive transport is simulated in the traveltime domain, and predictions at particular observation planes are obtained by weighting the concentration computed at each traveltime with the probability density of that traveltime in the observation plane and integration over the entire range of traveltimes [*Simmons et al.*, 1995; *Ginn et al.*, 1995; *Cirpka and Kitanidis*, 2001]. The *pdf* of traveltime may be directly taken from a conservative-tracer experiment or parameterized by appropriate distribution functions.

[14] The advective-dispersion streamtube model of *Cirpka and Kitanidis* [2000a] may be seen as an extension of the stochastic-convective approach. Here longitudinal dispersive mixing is accounted for. To distinguish between dispersive mixing from solute spreading, point-like measured BTCs of conservative tracers are analyzed. *Cirpka* [2002] demonstrated that effective dispersion coefficients for point-like injection, derived from first-order stochastic theory [*Dentz et al.*, 2000; *Fiori and Dagan*, 2000] may be used as mixing-related dispersion coefficients. The approach has been successfully applied to bioreactive transport by *Janssen et al.* [2006]. *Ginn* [2001] presented a similar approach allowing longitudinal dispersion in a single streamtube, which was applied to simulate an intermediate-scale biodegradation experiment [*Ginn et al.*, 2001]. Unlike the advective-reactive transport in the stochastic-convective framework, the approaches of *Cirpka and Kitanidis* [2000b] and *Ginn* [2001] solve advective-dispersive-reactive transport in each streamtube. In the advective-dispersion streamtube model, the BTC of a conservative tracer observed in an observation plane cannot be directly considered as the traveltime *pdf* because it reflects both advection and dispersion. Instead, a corrected traveltime *pdf* reflecting the impact of advection alone on the BTC, denoted advective traveltime *pdf*, is used. *Cirpka and Kitanidis* [2000b] assumed an inverse-Gaussian distribution to describe the advective traveltime *pdf*, and applied the method of temporal moments to approximate it. Gaussian, lognormal and gamma distributions have also been employed to characterize the traveltime *pdf* [*Simmons*, 1982; *Shapiro and Cvetkovic*, 1990; *Rubin and Dagan*, 1992; *Simic and Destouni*, 1999; *Loaiciga*, 2004; *Luo et al.*, 2006]. In addition, particle tracking schemes have been applied to derive traveltime statistics [e.g., *Bellin et al.*, 1994; *Selroos and Cvetkovic*, 1992; *Selroos*, 1995; *Hassan et al.*, 2001].

[15] The stochastic-convective model with kinetic mass transfer assumes advective-reactive transport in the mobile phase interacting with an immobile phase by kinetic mass transfer. This model is well suited to describe transport of sorbing compounds and transport in mobile-immobile aquifers. The traveltime *pdf* of a compound, subject to both transport in the mobile phase and retention in the immobile phase, can be expressed as a function of the traveltime *pdf* resulting from transport only in the mobile phase, also called as transition-time *pdf* [*Cvetkovic and Haggerty*, 2002], in the Laplace domain [*Villermaux*, 1987; *Sardin et al.*, 1991]. This concept has been applied to study anomalous transport [*Dentz and Berkowitz*, 2003; *Margolin et al.*, 2003], to characterize breakthrough tailing [*Cvetkovic and Haggerty*, 2002], to describe transport coupled to sorption/desorption [*Cvetkovic et al.*, 1998; *Lawrence et al.*, 2002; *Dentz and Berkowitz*, 2003], and to simulate geochemical reactive transport [*Rubin et al.*, 1997]. First-order, diffusive, and multirate models, among others, are available to describe the mass exchange between the mobile and immobile phases [e.g., *Chen and Wagenet*, 1995; *Haggerty and Gorelick*, 1995, 1998]. In addition, the model has been extended to include spatial variability of hydraulic conductivity and geochemical parameters [*Cvetkovic and Dagan*, 1994; *Cvetkovic et al.*, 1998]. A restriction of the model is that it assumes that all spatial parameters can be associated with traveltimes, thus it requires correlations between traveltime and reactive parameters. If reactive parameters and

traveltimes cannot be mapped to each other, the entire joint *pdf* of traveltime and reactive parameters must be sampled to predict the concentration of a reactive compound at a desired observation point. The stochastic-convective model with mass transfer neglects local dispersion, but uses the mass exchange between the mobile and immobile phase to account for mixing resulting from both local dispersion and kinetic mass transfer [*Simic and Destouni*, 1999]. Thus the general procedure to build such a model is to first approximate the advective traveltime *pdf*, and then to determine the mass transfer model and parameters [*Rubin and Ezzedine*, 1997; *Bellin and Rubin*, 2004]. Similar to the advective-dispersive streamtube model, local BTCs need to be measured to estimate the advective traveltime *pdf*. However, while in the advective-dispersive streamtube model the local BTCs are used to estimate apparent local mixing parameters, the stochastic-convective model with mass transfer uses the local information to directly parameterize the advective traveltime *pdf* [*Rubin and Ezzedine*, 1997; *Woodbury and Rubin*, 2000].

[16] The traveltime-based models discussed above are convenient to simulate BTCs measured at certain observation points and control planes where tracer concentration BTCs are measured. In order to make predictions at points where tracer measurements are not available, spatial distributions of traveltimes must be estimated, which may be attained by the streamline-method of *Crane and Blunt* [1999], among others. The streamline method also transforms multidimensional spatial coordinates to one-dimensional traveltime coordinates. However, in contrast to the traveltime methods discussed above, the streamline method aims to simulate the actual spatial distribution of concentration and thus requires determining the distribution of streamlines and computing the traveltime distribution along each of them. *Obi and Blunt* [2004] also extended the streamline-method to model diffusion and dispersion in solute transport problems using an operator splitting technique where dispersive transport is solved on an underlying spatial grid. Spatial aquifer characterizations may be associated with traveltimes to estimate spatial distributions of traveltimes [e.g., *Datta Gupta et al.*, 2002]. Interpolating traveltime distributions between observation points requires an excellent spatial coverage of the domain. This is equivalent to calibrating a spatially explicit model. If main features of the domain are not identified, the predicted traveltime distributions will be biased. For the prediction of BTCs of reactive compounds from those of conservative components at a given observation point, by contrast, the spatial coverage is not necessary.

3. Transport Model in Spatial Coordinates

3.1. Governing Equations

[17] We consider multidimensional advective-dispersive transport of a compound undergoing first-order kinetic mass transfer between the mobile and a single immobile domain in an initially tracer-free heterogeneous media [e.g., *Coats and Smith*, 1964]:

$$\theta_m \frac{\partial c_m}{\partial t} + \mathbf{q} \cdot \nabla c_m \quad \nabla \cdot (\theta_m \mathbf{D} \nabla c_m) = \alpha (c_i \quad c_m) \qquad (1)$$

Eawag 05291

$$\theta_i \frac{\partial c_i}{\partial t} = \alpha (c_m \quad c_i) \qquad (2)$$

with the mobile and immobile porosities θ_m and θ_i, respectively, the specific discharge vector $\mathbf{q}$, the first-order rate coefficient α of mass transfer between the mobile and immobile domain, and the dispersion tensor $\mathbf{D}$:

$$\theta_m \mathbf{D} = \frac{\mathbf{q} \otimes \mathbf{q}}{\|\mathbf{q}\|} (k_\ell \quad k_t) + \mathbf{I}(k_t \|\mathbf{q}\| + \theta_m D_e) \qquad (3)$$

in which k_ℓ and k_t are the longitudinal and transverse dispersivities of the porous medium, respectively, $\mathbf{q} \otimes \mathbf{q}$ denotes the matrix product of vector $\mathbf{q}$ with itself, $\mathbf{I}$ is the identity matrix, and D_e is the pore-diffusion coefficient of the transported compound.We specify initial concentrations of zero within the domain:

$$c(\mathbf{x}, t = 0) = c_{im}(\mathbf{x}, t = 0) = 0. \qquad (4)$$

[18] A uniform tracer pulse is instantaneously injected into the domain over the inflow boundary Γ_{in}:

$$\mathbf{n} \cdot (\mathbf{v}c \quad \mathbf{D} \nabla c) = \frac{m_{in}}{Q} \delta(t) \mathbf{n} \cdot \mathbf{v} \text{ on } \Gamma_{in} \qquad (5)$$

where m_{in} is the mass of the injected solute, and Q is the total discharge crossing the inflow boundary Γ_{in}. At all other parts of the boundary, denoted $\Gamma \backslash \Gamma_{in}$, the dispersive flux normal the boundary is zero:

$$\mathbf{n} \cdot (\mathbf{D} \nabla c) = 0 \text{ on } \Gamma \backslash \Gamma_{in} \qquad (6)$$

Laplace transformation of equations (1) and (2) yields:

$$\theta_m s \tilde{c}_m + \mathbf{q} \cdot \nabla \tilde{c}_m \quad \nabla \cdot (\theta_m \mathbf{D} \nabla \tilde{c}_m) = \alpha (\tilde{c}_i \quad \tilde{c}_m) \qquad (7)$$

$$\theta_i s \tilde{c}_i = \alpha (\tilde{c}_m \quad \tilde{c}_i) \qquad (8)$$

in which s is the complex coordinate in the Laplace domain, and quantities with a tilde are Laplace transforms of the corresponding time functions. Rearranging equation (8) yields:

$$\tilde{c}_i = \frac{1}{\tau_{ad} s + 1} \tilde{c}_m \qquad (9)$$

in which τ_{ad} is the characteristic time of sorption, defined by:

$$\tau_{ad} = \frac{\theta_i}{\alpha} \qquad (10)$$

Substituting equation (9) into equation (7) and rearranging terms gives [e.g., *Sardin et al.*, 1991]:

$$\mathbf{q} \cdot \nabla \tilde{c}_m \quad \nabla \cdot (\theta_m \mathbf{D} \nabla \tilde{c}_m) = \quad (M + 1) s \theta_m \tilde{c}_m \qquad (11)$$

with the memory function M:

$$M = \frac{\kappa}{\tau_{ad} s + 1} \tag{12}$$

and the capacity term κ:

$$\kappa = \frac{\theta_i}{\theta_m} \tag{13}$$

[19] For other linear kinetic mass transfer models, such as that based on diffusion into spheres, the memory function differs from equation (12), whereas equation (11) is identical [e.g., *Sardin et al.*, 1991].

3.2. Effects of Processes Considered

[20] *Hydraulic heterogeneity* of the formation leads to a spatially varying specific-discharge field $\mathbf{q}(\mathbf{x})$ and thus to nonuniform advection. As a result, a solute cloud introduced into the domain becomes increasingly irregular in shape. The parts of the plume that are in high-velocity regions over a certain period of time are sheared off from the parts in low-velocity regions. As a consequence, the plume boundary, exhibiting sharp concentration gradients, increases in size. Classical stochastic subsurface theory has analyzed the spatial moments of extended plumes and matched them with macrodispersion equations, which are Fickian in the large-time limit (see the textbooks of *Dagan* [1989], *Gelhar* [1993], and *Rubin* [2003]). The amount of spreading experienced by a plume undergoing strictly advective transport in a heterogeneous domain depends on the size of the plume [e.g., *Kitanidis*, 1988]. At the limit of point-like injection, no spreading would occur at all, that is, the plume would remain a Dirac pulse [e.g., *Dentz et al.*, 2000]. In such a situation, however, the exact travel distance passed by the point-like plume would depend on the exact starting location, and the uncertainty of locating the plume position could be expressed by macrodispersion expressions [e.g., *Fiori and Dagan*, 2000].

[21] If we consider two adjacent extended solute plumes undergoing advection in a heterogeneous formation, the spatially variable velocity field would make the interface between the two plumes increasingly irregular, and its surface area would increase. The two plumes, however, would not mix. That is, although the macroscopic description of solute transport by macrodispersion may be adequate, the unresolved variations of the concentration distributions would result in strict separation of the plumes. This has serious implications for upscaling of transport when compounds are considered that react with each other [*Kapoor et al.*, 1997].

[22] *Local longitudinal dispersion* smears the concentration distribution along individual streamlines. If we consider two solute clouds introduced into the domain one after the other, they start to overlap at the interface. Overall, however, the effect of local longitudinal dispersion on macroscopic transport in heterogeneous domains is of minor importance. *Local transverse dispersion*, by contrast, significantly contributes to solute mixing in heterogeneous formations. The new interfacial area, created by heterogeneity, is mainly aligned with the direction of flow, facilitating enhanced transverse exchange. As visual example, transverse dispersion transfers solute mass from the tips of advancing plume fringes to the surrounding, yet solute free, region [e.g., *Janssen et al.*, 2006, Figure 1]. In the replacement setup mentioned above, this may lead to macroscopically longitudinal mixing of the two solute clouds, which is stronger than the mixing caused by local longitudinal dispersion, although the local transverse dispersivities are typically assumed to be about an order of magnitude smaller than the longitudinal counterparts.

[23] In the analysis of point-like observations of solute breakthrough, longitudinal dispersion does not alter the mean breakthrough time at any location, whereas transverse dispersion balances differences of mean breakthrough time between adjacent streamtubes in heterogeneous formations. Both processes lead to wider local BTCs. Thus a particular set of point-like measured BTCs within an observation plane may be interpreted as caused by transport with transverse dispersion in a highly variable velocity field or by transport with enhanced longitudinal dispersion rather than transverse exchange, but in a less variable velocity field. This ambiguity is used in the advective-dispersive streamtube approach [*Cirpka and Kitanidis*, 2000a, 2000b; *Cirpka*, 2002; *Janssen et al.*, 2006].

[24] Like local longitudinal dispersion, kinetic mass transfer leads to mixing along individual streamlines. In fact, kinetic mass transfer models have been used as an alternative parameterization of longitudinal dispersion [e.g., *Brusseau*, 1992]. The two-domain model, listed above, can lead to BTCs that are similar to those obtained by one-dimensional advective-dispersive transport in cases where the characteristic time τ_{ad} of sorption is considerably smaller than the mean breakthrough time. Large values of τ_{ad} lead to strong tailing. A concentration spike may occur at the advective traveltime when local dispersion is small and the characteristic time τ_{ad} of sorption is large. In this regime, the development of two peaks is possible [*Quinodoz and Valocchi*, 1993; *Michalak and Kitanidis*, 2000]. Kinetic mass transfer can be an efficient longitudinal mixing mechanism. It contributes to transverse mixing only in case of transient flow [*Cirpka*, 2005]. In the replacement setup mentioned above, remnants of the receding solution still exists in the immobile domain at times when the invading solution is already in the mobile domain.

4. Streamline Representation

4.1. Transport Along Individual Streamlines

[25] In the following approximations, transverse dispersion is not accounted for explicitly. Conceptually, transport is restricted to the longitudinal direction, that is, along independent streamlines. In this framework, the expected concentration obtained in an extended observation plane is computed by integrating the solute flux of all streamlines crossing the observation plane (see below). The effect of local transverse dispersion on longitudinal transport must be accounted for by modifying the remaining coefficients (i.e., decrease of variability in q, increase of either D_ℓ or κ and τ_{ad}, or a combination of those modifications). The transport equation along an individual streamline is now:

$$\theta_m \frac{\partial c_m}{\partial t} + q(x_\ell) \frac{\partial c_m}{\partial x_\ell} \quad \frac{\partial}{\partial x_\ell}\left(\theta_m D_\ell \frac{\partial c_m}{\partial x_\ell}\right) = \alpha(c_i \quad c_m) \tag{14}$$

Table 1. Characteristics of Simplified Streamline Transport Models Eawag 05291

Model	Memory Function	Inverse Peclet Number	Solution in Laplace Domain	Solution in Time Domain
Advective-dispersive streamtube approach	M 0	$\varepsilon > 0$	c_m $\exp\left(\frac{2s}{1+\sqrt{1+4\tau\varepsilon s}}\tau\right)$	Numerical inverse Laplace transformation
Stochastic-convective transport with mass transfer	$M(s)$ / 0	ε 0	c_m exp(s(1 + M) τ)	
Stochastic-convective transport without mass transfer	M 0	ε 0	c_m exp($s\tau$)	c_m δ (t τ)

in which x_ℓ is the streamline coordinate, and D_ℓ is the effective longitudinal dispersion coefficient.

[26] We may change from the longitudinal spatial coordinate x_ℓ to advective traveltime τ:

$$\tau = \int_0^x \frac{\theta_m dx_\ell}{q(x_\ell)} \tag{15}$$

If we also approximate that the effective dispersion coefficient D_ℓ is uniform, we arrive at:

$$\frac{\partial c_m}{\partial t} + \frac{\partial c_m}{\partial \tau} \quad \varepsilon\tau \frac{\partial^2 c_m}{\partial \tau^2} = \frac{\kappa}{\tau_{ad}}(c_i \quad c_m) \tag{16}$$

in which ε is the inverse Peclet number:

$$\varepsilon = \frac{\theta_m D_\ell}{q x_\ell} \tag{17}$$

[27] It should be worth noting that stochastic transport theory clearly results in effective dispersion coefficients increasing with travel distance until an asymptotic value is reached at late times for mean uniform flow in an infinite domain [e.g., *Dentz et al.*, 2000], whereas equation (16) is based on uniform longitudinal dispersion. Thus the inverse Peclet number ε used in this equation is an apparent variable, expressing how an observed point-related BTC resulting from multidimensional transport in a heterogeneous domain can be described as if caused by one-dimensional transport with uniform coefficients [e.g., *Cirpka and Kitanidis*, 2000a]. Obviously, ε determined for a certain travel distance must not be applied to other travel distances.

[28] Laplace transformation of equation (16) and consideration of equation (9) yields:

$$\frac{d\tilde{c}_m}{d\tau} \quad \varepsilon\tau \frac{d^2\tilde{c}_m}{d\tau^2} = \quad (M+1)s\tilde{c}_m \tag{18}$$

which is a one-dimensional steady-state transport equation with first-order source/sink term. Considering a unit-pulse input of $c_m(x = 0, t) = \delta(t)$ as boundary condition in the time domain, the Laplace-domain solution becomes [e.g., *Sardin et al.*, 1991]:

$$\tilde{c}_m = \exp\left(\quad \frac{2s(1+M)}{1+\sqrt{1+4\tau\varepsilon s(1+M)}}\tau \right) \tag{19}$$

[29] To obtain the time domain BTC $c_m(\tau, t)$ of an individual streamline with advective traveltime τ, equation (19) needs to be transformed back into the time domain, which is done most easily by numerical methods.

4.2. Ensemble of Streamlines

[30] We now consider the BTC obtained at an extended observation plane. We denote this BTC as an integrated one, in contrast to local ones that would be observed at idealized points. The integrated BTC is the weighted average concentration of all streamlines crossing the observation plane, or ending in the well. In the formulation given above, the only difference between the various streamlines connecting the injection and observation area lies in the advective traveltime τ. All other transport parameters are assumed to be identical. Then, the weight that is given to the BTC with a particular advective traveltime τ is identical to the probability density of the traveltime, which equals the volumetric fraction of water with advective traveltime τ in the mixture of contributions with various values of τ. The expected concentration $C(L, t)$ at an observation time t is given by integrating the weighted concentrations of all streamtubes over the traveltime:

$$C(L,t) = \int_0^\infty c_m(\tau,t)p(\tau)d\tau \tag{20}$$

where $p(\tau)$ is the traveltime *pdf*. C aims to represent the flux-integrated BTC.

4.3. Simplified Streamline Transport

[31] The model is composed of equations (19) and (20) can be conveniently simplified to the models summarized in Table 1. For the advective-dispersive streamtube approach in which only a mobile domain is considered, spreading of local BTCs is assigned to apparent longitudinal dispersion exclusively. This model cannot reproduce local BTCs with strong tailing. For the stochastic-convective model, no longitudinal dispersion is considered. When it is combined with a two-domain model, the effects of transverse mixing on local BTCs is attributed to mobile-immobile exchange. Thus direct measurements of κ and τ_{ad} at the local scale, e.g., by core studies, cannot be applied to macroscopic transport. Also, BTCs computed for individual streamlines $c_m(\tau, t)$ exhibit a distinct spike at $t = \tau$ if $\tau_{ad} > \tau$. Such spikes may not be observed in measurements. When kinetic mass transfer is also neglected, C is interpreted as probability density function of advective traveltimes $p(\tau)$. The latter model does not allow for any mixing.

4.4. Parameters Describing Local Mixing

[32] For the mixing models based on traveltimes proposed in this study, we have two groups of parameters to be estimated: those describing mixing processes, namely

Table 2. Mixing Parameters as a Function of Temporal Moments of Local Breakthrough Curves Eawag 05291

Model	Apparent Inverse Peclet Number, $\langle\varepsilon\rangle$	Apparent Capacity, $\langle\kappa\rangle$	Apparent Characteristic Timescale, $\langle\tau_{ad}\rangle$
Advective-dispersive streamtube approach	$\langle\varepsilon\rangle \quad \left\langle \frac{m_0 m_{2c}}{2m_1^2} \right\rangle$	0	0
Stochastic-convective transport with mass transfer	0	$\langle\kappa\rangle \quad \left\langle \frac{3m_{2c}^2}{2m_1 m_{3c} - 3m_{2c}^2} \right\rangle$	$\langle\tau_{ad}\rangle \quad \left\langle \frac{1}{3}\frac{m_{3c}}{m_{2c}} \right\rangle$
Advective-dispersive streamtube with mass transfer	$\langle\varepsilon\rangle \quad \left\langle \frac{m_0 m_{2c}}{2m_1^2} \quad \frac{\kappa\tau_{ad}}{\kappa+1}\frac{m_0}{m_1} \right\rangle$	κ	τ_{ad}

kinetic mass transfer, κ and τ_{ad}, and dispersive mixing, ε; and the traveltime distribution $p(\tau)$. The spread and tailing of local BTCs are considered to primarily result from the mixing processes, while the integrated BTC is influenced by both mixing processes and spreading caused by heterogeneous advection, which is represented here by $p(\tau)$. Thus we suggest the following procedure for parameter estimation: (1) estimating the mixing parameters from core samples or local BTCs; and (2) determining the traveltime distribution from the integrated BTC and the estimated mixing parameters. With respect to different traveltime-based models, different mixing parameters and traveltime distributions should be applied. The mixing parameters can be expressed as functions of the temporal moments of local BTCs.

[33] Raw temporal moments of concentration BTCs are defined by:

$$m_k(\mathbf{x}) = \int_0^\infty t^k c_m(\mathbf{x}, t) dt \tag{21}$$

and central moments by:

$$m_{kc}(\mathbf{x}) = \int_0^\infty \left(t \quad \frac{m_1}{m_0} \right)^k c_m(\mathbf{x}, t) dt \tag{22}$$

which can be computed from raw moments by:

$$\frac{m_{2c}}{m_0} = \frac{m_2}{m_0} \quad \left(\frac{m_1}{m_0}\right)^2 \tag{23}$$

$$\frac{m_{3c}}{m_0} = \frac{m_3}{m_0} \quad 3\frac{m_2 m_1}{(m_0)^2} + 2\left(\frac{m_1}{m_0}\right)^3 \tag{24}$$

[34] Analytical expressions for temporal moments as functions of the mixing parameters are given by *Kreft and Zuber* [1978], *Valocchi* [1989], *Cunningham and Roberts* [1998], among others. Table 2 summarizes the equations to evaluate the mixing parameters for the traveltime-based models. Angle brackets denote mean values of expressions evaluated from moments of local BTCs. For the advective-dispersive streamtube approach with mass transfer, one may describe the mixing caused by transverse dispersion either by longitudinal dispersion or by kinetic mass transfer. Here we assume the correct description of mixing caused by kinetic mass transfer, which may be obtained by core-sample experiments, and the effect of transverse mixing across streamlines are parameterized by longitudinal dispersion. As an alternative, one can surely assume apparent mass transfer parameters and true local longitudinal dispersion. For small local dispersion coefficients, the latter will be similar to the case in which dispersion is completely neglected, i.e., the stochastic-convective transport model with mass transfer. Estimating both apparent dispersion and mass transfer parameters from local BTCs will require even higher-order moments which are highly unreliable in practice. Note that the three models represent three different characterizations of mixing although all are based on temporal moments of local BTCs: the advective-dispersive streamtube approach describes mixing completely by longitudinal dispersion; the stochastic-convective transport model with mass transfer by kinetic mass transfer; and the final one can be considered as a combination of the first two.

5. Inference of Advective Travel-Time Distribution

[35] The critical point for designing a traveltime-based model is to estimate the traveltime distribution. As already mentioned, *Cirpka and Kitanidis* [2000b] assumed an inverse-Gaussian distribution to describe the advective traveltime *pdf* $p(\tau)$, and applied the method of temporal moments to approximate it. A major drawback of evaluating the parameters of a parametric function for $p(\tau)$ is that the shape of $p(\tau)$ is predefined. For instance, the best distribution may exhibit multiple peaks, but the parametric model may be unimodal. In that case it would by construction be impossible to obtain a multimodal distribution. Such limitations can be overcome when we allow $p(\tau)$ to adapt freely to the needs of the problem. We do this by estimating a set $p(\tau_j)$ of probability densities of discrete advective traveltimes τ_j from the measured integrated BTC $C(L, t)$ using minimal prior information. The approach is a modification of that of *Cirpka et al.* [2007], derived for deconvolution of time series.

[36] Discretizing time t and advective traveltime τ in equation (20) yields:

$$C(L, t_i) \approx \sum_{j\ 0}^{n_\tau} c_m(\tau_j, t_i) p(\tau_j) \Delta\tau \tag{25}$$

$$\mathbf{C} = \mathbf{X}\mathbf{p} \tag{26}$$

with

$$X_{ij} = \Delta\tau c_m(\tau_j, t_i) \tag{27}$$

in which $c_m(\tau_j, t_i)$, and thus $\mathbf{X}$, depends on the transport and mass transfer parameters ε, κ, and τ_{ad}, which are assumed to be uniform and identical along all streamlines.

Eawag 05291

[37] For regularization, we assume that $p(\tau)$ is a second-order intrinsic autocorrelated time function with multi-Gaussian prior probability density function and a linear variogram:

$$p(\tau) = \beta + p'(\tau) \tag{28}$$

$$E[p'(\tau)] = 0 \forall \tau \tag{29}$$

$$E\left[\frac{1}{2}(p'(\tau+h) \quad p'(\tau))^2\right] = \gamma_p(h) = \theta|h| \tag{30}$$

in which β is the (unknown) mean value of $p(\tau)$, $p'(\tau)$ is the deviation from the mean, $\gamma_p(h)$ is the semi-variogram, and θ is the slope of the linear variogram function.Then, the vector $\mathbf{p}$ of discrete values of $p(\tau)$ has the following prior statistics:

$$E[\mathbf{p}] = \mathbf{u}\beta \tag{31}$$

$$E[\mathbf{p}' \otimes \mathbf{p}'] = a \quad \Gamma_{\mathbf{pp}} \tag{32}$$

in which $\mathbf{u}$ is a vector of unit entries, $\Gamma_{\mathbf{pp}}$ is the semivariogram matrix, and a is a constant.

[38] We assume that the likelihood of the vector $\mathbf{C}$ of measured concentration values follows a Gaussian distribution, and that the error of the individual measurements is uncorrelated, resulting in a quadratic expression of the log likelihood $L(\mathbf{C}|\mathbf{p}', \beta)$:

$$L(\mathbf{C}|\mathbf{p}', \beta) = \frac{(\mathbf{C} \quad \mathbf{X}(\mathbf{p}' + \mathbf{u}\beta)) \cdot (\mathbf{C} \quad \mathbf{X}(\mathbf{p}' + \mathbf{u}\beta))}{\sigma_{ep}^2} \tag{33}$$

in which σ_{ep}^2 is variance of the measurements expressing epistemic error. The epistemic error includes the error of the measurement procedure and the error resulting from applying a potentially wrong model.

[39] In order to infer the parameters $\mathbf{p}'$ and β, we use Bayes' theorem, yielding for the posterior log likelihood of $\mathbf{p}'$ and β given $\mathbf{C}$:

$$\begin{aligned} L(\mathbf{p}', \beta|\mathbf{C}) &= L(\mathbf{C}|\mathbf{p}', \beta) + L(\mathbf{p}', \beta) \quad L(\mathbf{C}) = \\ &= \frac{(\mathbf{C} \quad \mathbf{X}(\mathbf{p}' + \mathbf{u}\beta)) \cdot (\mathbf{C} \quad \mathbf{X}(\mathbf{p}' + \mathbf{u}\beta))}{\sigma_{ep}^2} \quad \mathbf{p}'^T \Gamma_{\mathbf{pp}}^{-1} \mathbf{p}' \\ &\quad + const. \end{aligned} \tag{34}$$

[40] In our estimation we minimize $L(\mathbf{p}', \beta|\mathbf{C})$, which results in a smooth distribution of $\mathbf{p}'$. Since $p(\tau)$ is a probability density, it must not become negative. Also, the integral of $p(\tau)$ in the bounds of $\tau = 0$ to the maximum advective traveltime $\tau_{\max}$ considered must not become larger than unity. These two conditions lead to the following constraints:

$$\mathbf{p} = \mathbf{p}' + \mathbf{u}\beta \geq \mathbf{0} \tag{35}$$

$$\mathbf{p} \cdot \mathbf{u}\Delta\tau = \mathbf{p}' \cdot \mathbf{u}\Delta\tau + n_\tau \Delta\tau\beta \leq 1 \tag{36}$$

[41] Equation (35) is an inequality constraint. Only when a certain element of $\mathbf{p}$ becomes negative in the estimation procedure, the constraint has to be activated. We may express this by:

$$\mathbf{H}(\mathbf{p}' + \mathbf{u}\beta) = \mathbf{0} \tag{37}$$

in which $\mathbf{H}$ is a $n_\upsilon \times n_g$ selection matrix with n_υ being the number of active constraints:

$$H_{ij} = \begin{cases} 1 \text{ if } p_i \text{ is affected by the } i \quad \text{th constraint} \\ 0 \text{ otherwise} \end{cases} \tag{38}$$

[42] Likewise, equation (36) has to be activated when $\mathbf{p} \cdot \mathbf{u}\Delta\tau$ becomes larger than unity without the constraint. Accounting for the constraints can be achieved by the method of Lagrange multipliers [e.g., *Vogel*, 2002, Chapter 9]. Then, the constrained minimization of $L(\mathbf{p}', \beta|\mathbf{C})$ consists of solving the following system of linear equations:

$$\begin{bmatrix} \frac{1}{\sigma_{ep}^2}\mathbf{X}^T\mathbf{X} & \Gamma_{\mathbf{ff}}^{-1} & \frac{1}{\sigma_{ep}^2}\mathbf{X}^T\mathbf{X}\mathbf{u} & \mathbf{H}^T & \Delta\tau\mathbf{u} \\ \frac{1}{\sigma_{ep}^2}\mathbf{u}^T\mathbf{X}^T\mathbf{X} & & \frac{1}{\sigma_{ep}^2}\mathbf{u}^T\mathbf{X}^T\mathbf{X}\mathbf{u} & \mathbf{u}_\upsilon^T & n_\tau\Delta\tau \\ \mathbf{H} & & \mathbf{u}_\upsilon & \mathbf{0} & \mathbf{0} \\ \Delta\tau\mathbf{u}^T & & n_\tau\Delta\tau & \mathbf{0} & 0 \end{bmatrix} \begin{bmatrix} \mathbf{p}' \\ \beta \\ \upsilon \\ \mu \end{bmatrix} = \begin{bmatrix} \frac{1}{\sigma_{ep}^2}\mathbf{X}^T\mathbf{C} \\ \frac{1}{\sigma_{ep}^2}\mathbf{u}^T\mathbf{X}^T\mathbf{C} \\ \mathbf{0} \\ 1 \end{bmatrix} \tag{39}$$

in which υ is the $n_\upsilon \times 1$ vector of Lagrange multipliers, and $\mathbf{u}_\upsilon$ is a $n_\upsilon \times 1$ vector of unit entries. Activation and deactivation of the constraints depend on the behavior of the solution. The following rules apply for the non-negativity constraints:

[43] $p_j < 0 \rightarrow$ add constraint for element j

[44] $\upsilon_i \leq 0 \rightarrow$ keep constraint i

[45] $\upsilon_i > 0 \rightarrow$ remove constraint $i$and for the integral constraint:

$$\Delta\tau \sum_{i\ 1}^{n_\tau} p_i > 1 \rightarrow \text{activate the integral constraint} \tag{40}$$

$$\mu \geq 0 \rightarrow \text{keep the integral constraint;} \tag{41}$$

$$\mu < 0 \rightarrow \text{remove the integral constraint} \tag{42}$$

in which removing the integral constraints consists of removing the last row and column in the left-hand side matrix, the variable μ, and the last element of the right-hand side vector in equation (39).

[46] The epistemic error, assumed identical for all measurements, can be estimated by enforcing that the sum of squared residuals, weighted by their variance σ_{ep}^2, meets its expected value (see study by *Press et al.* [1992], equation 15.1.6)):

$$\sigma_{ep}^2 = \frac{(\mathbf{C} \quad \mathbf{X}(\mathbf{p}' + \mathbf{u}\beta)) \cdot (\mathbf{C} \quad \mathbf{X}(\mathbf{p}' + \mathbf{u}\beta))}{n_t \quad n_\tau + n_\upsilon + n_\mu \quad 1} \tag{43}$$

in which $n_t - n_\tau + n_\upsilon + n_\mu - 1$ corresponds to the degrees of freedom in estimating $\mathbf{p}$ from $\mathbf{C}$, subject to n_υ active nonnegativity constraints and n_μ integral constraints. This approach is well accepted in optimization of overdetermined problems.

[47] The estimation of $\mathbf{p}$ has to be repeated until the Lagrange multipliers don't differ any more from one iteration to the next. In this case, all necessary constraints have been identified. In each iteration, the epistemic error σ_{ep}^2 is evaluated after updating $\mathbf{p}$.

[48] *Cirpka et al.* [2007] also demonstrated how the slope θ of the variogram can be estimated from the data. Such analysis, however, is beyond the scope of the present study.

6. Reactive Transport

[49] In the previous sections, we have only considered transport of a conservative tracer. Here we extend the analysis to multicomponent reactive transport coupled to mobile-immobile mass transfer. Denoting the mobile- and immobile-phase concentrations of compound j by $c_m^{(j)}$ and $c_i^{(j)}$, respectively, the reactive transport equation for that compound reads in spatial coordinates:

$$\theta_m \frac{\partial c_m^{(j)}}{\partial t} + \mathbf{q} \cdot \nabla c_m^{(j)} \quad \nabla \cdot \left(\theta_m \mathbf{D} \nabla c_m^{(j)} \right) = \alpha \left(c_i^{(j)} \quad c_m^{(j)} \right) + r_m^{(j)} \tag{44}$$

$$\theta_i \frac{\partial c_i^{(j)}}{\partial t} = \alpha \left(c_m^{(j)} \quad c_i^{(j)} \right) + r_i^{(j)} \tag{45}$$

in which $r_m^{(j)}$ and $r_i^{(j)}$ are reaction rates in the mobile and immobile phases depending on the concentrations of all compounds in the particular phase at a given time and location.

[50] In the traveltime domain, equation (44) is replaced by the reactive analogue to equation (16):

$$\frac{\partial c_m^{(j)}}{\partial t} + \frac{\partial c_m^{(j)}}{\partial \tau} \quad \varepsilon\tau \frac{\partial^2 c_m^{(j)}}{\partial \tau^2} = \frac{\kappa}{\tau_{ad}} \left(c_i^{(j)} \quad c_m^{(j)} \right) + r_m^{(j)} \tag{46}$$

whereas the governing equation for the concentration in the immobile phase, equation (45), is not altered. In addition to the assumptions made for formulating conservative-tracer transport in traveltime coordinates, it must be permissible to map reaction rates from the spatial domain to the traveltime domain, i.e., $r_m^{(j)}(\mathbf{x}, t) = r_m^{(j)}(\tau(\mathbf{x}), t)$ and $r_i^{(j)}(\mathbf{x}, t) = r_i^{(j)}(\tau(\mathbf{x}), t)$. The latter condition is met in most self-organizing reactive systems, where reaction rates depend on concentration but not on material properties that vary independent off the reaction in space [e.g., *Cirpka and Kitanidis*, 2001; *Janssen et al.*, 2006].

[51] In general, solving equations (45) and (46) for a particular set of mixing-related coefficients, ε, κ, and τ_{ad}, applying a particular reaction model, cannot be simplified by transformation into the Laplace domain, as done for conservative-tracer transport. That is, equations (45) and (46) must be solved numerically using standard discretization method in time and traveltime.

[52] The flux-averaged concentration $C^{(j)}(L, t)$ of reactive compound j in the outflow is computed from the concentrations $c_m^{(j)}(\tau, t)$ of the reactive compound depending on time and traveltime according to:

$$C^{(j)}(L,t) = \int_0^\infty c_m^{(j)}(\tau, t) p(\tau) d\tau \tag{47}$$

which is equivalent to equation (20) in conservative-tracer transport. $C^{(j)}(L, t)$ depends on reactive parameters, the mixing-related coefficients, ε, κ, and τ_{ad}, and on the advective traveltime distribution $p(\tau)$ in the outflow. In the transfer from conservative to reactive transport, we estimate the mixing-related coefficients from local BTCs of the conservative tracer and the traveltime distribution $p(\tau)$ from the integrated BTC of the conservative tracer subject to the particular set of mixing-related coefficients. The reactive parameters, determining chemical transformation rates, must be identified by independent studies, e.g., in the lab.

7. Two-Dimensional Test Cases

7.1. Numerical Methods

[53] We consider a two-dimensional test case representing transport in a periodic heterogeneous aquifer in which mean flow is in direction x_1. The length and width of the domain are $10m$ and $5m$, respectively. We consider a single realization of log hydraulic conductivity following an anisotropic, non-separable exponential covariance model. The geometric mean of hydraulic conductivity and variance of the log conductivity are $1 \times 10^{-4} m/s$ and 2, respectively. The integral scale is $0.8m$ in the longitudinal and $0.1m$ in the transverse direction. All parameters are listed in Table 3. The distribution of log conductivities is generated using the spectral method of *Dykaar and Kitanidis* [1992] on a rectangular 1000×500 cell grid (Figure 1a). The steady-state flow field is solved for a mean hydraulic gradient of 0.01 along x_1. A streamline-oriented grid for transport with grid resolution identical to that of the rectangular grid is generated using the streamline method of *Cirpka et al.* [1999c] (flow net shown in Figure 1b). The flow rate in each streamtube is identical. The dispersivities are $0.01m$ and $0.001m$ in the longitudinal and transverse direction, respectively. Kinetic mass transfer is described by a first-order mass transfer model with a constant mass transfer coefficient of $3 \times 10^{-7}/s$ and a uniform porosity of 0.2 for both the mobile and immobile regions. The numerical schemes for solving the transport problem have been presented elsewhere [*Cirpka et al.*, 1999a].

[54] Figure 2 shows the local and integrated BTCs at the outflow boundary for a conservative tracer with a Dirac delta input throughout the inflow boundary. The local BTCs are sampled from individual streamtubes, and the integrated BTC is the flux-averaged concentration of all streamtubes. Mean temporal moments of the local BTCs are listed in

Table 3. Parameters of the Two Dimensional Test Case

Parameter	Symbol	Values
Dimension of domain	$L_1 \times L_2$	$10m \times 5m$
Discretization	$\Delta x_1 \times \Delta x_2$	$0.01m \times 0.01m$
Covariance model		exponential
Correlation lengths	$\lambda_1 \times \lambda_2$	$0.8m \times 0.1m$
Variance of log conductivity	$\sigma_{\ln K}^2$	2
Geometric mean of conductivity	K_g	1×10^{-4} m/s
Mean hydraulic gradient	J	0.01
Mobile porosity	θ_m	0.2
Immobile porosity	θ_i	0.2
Rate coefficient of mass transfer	α	$3 \times 10^{-7}/s$
Dispersivities	$K_\ell \times k_t$	$0.01m \times 0.001m$
Pore diffusion coefficient	D	$1 \times 10^{-9} m^2/s$
Derived parameters of mass transfer		
Capacity term	κ	1
Characteristic time of mass transfer	τ_{ad}	$6.67 \times 10^5 s$
Moments of local and integrated BTCs in the outflow		
Mean local first moment	$\langle m_1^m \rangle$	$2.32 \times 10^6 s$
Mean second raw moment	$\langle m_2^m \rangle$	$1.09 \times 10^{13} s^2$
Mean local second central moment	$\langle m_{2c}^m \rangle$	$5.47 \times 10^{12} s^2$
Mean local third central moment	$\langle m_{3c}^m \rangle$	$5.83 \times 10^{18} s^3$

Table 3. The concentration peaks of the local BTCs spread out as a result of the heterogeneous conductivity field, while the peak of the integrated BTC appears at the time at which the majority of local breakthrough peaks. Long tails are observed at local BTCs because of the kinetic mass transfer. The long tail of the integrated BTC may result from both kinetic mass transfer and distributed traveltimes caused by heterogeneous advection.

7.2. Advective Travel-Time Distributions

[55] For the stochastic-convective model, the integrated BTC is directly considered as the advective traveltime

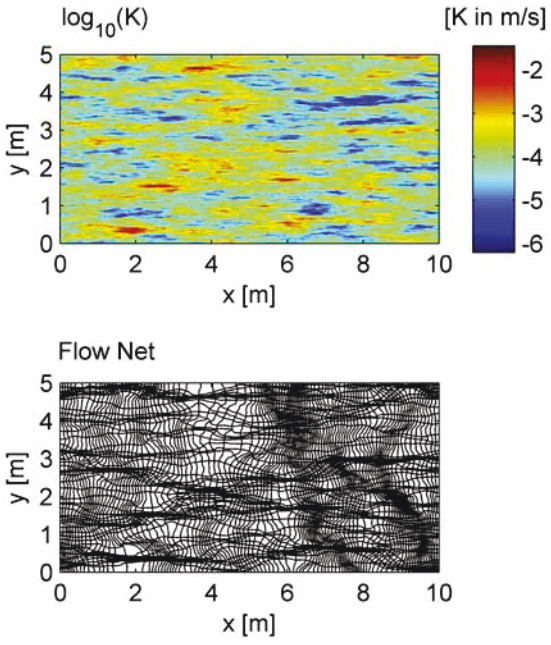

Figure 1. Two-dimensional heterogeneous hydraulic conductivity field used in the example calculation and resulting flow net.

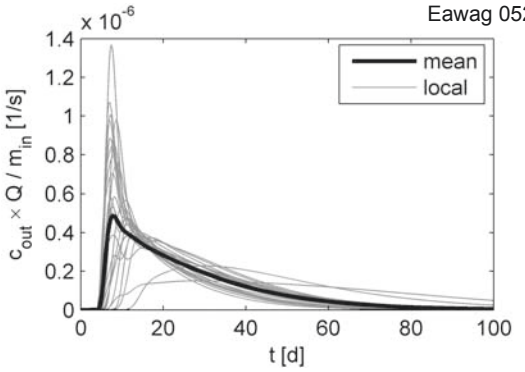

Figure 2. Integrated and local BTCs of a conservative tracer at the outflow boundary.

distribution, implying zero local mixing. For other traveltime-based models, Table 4 lists the mixing parameters estimated by the temporal moments of the local BTCs. The apparent mixing parameters are evaluated using the mean moments rather than the moments of mean concentrations, consistent to the approach for evaluating effective dispersion coefficients in heterogeneous media [*Cirpka and Kitanidis*, 2000b; *Dentz et al.*, 2000; *Cirpka*, 2002].

[56] Figure 3 shows the forward simulation results of the outflow BTCs for three cases, including (1) pure advection; (2) advection and local dispersion; and (3) advection, local dispersion, and mass transfer. It demonstrates that the pure advective traveltime distribution exhibits multimodal behavior, which is smoothed by dispersion and mass transfer. Thus, when the mixing mechanisms are separated from the integrated BTC, one may expect a multimodal advective traveltime distribution.

[57] Figure 4 shows the fitted advective traveltime distributions by the nonparametric method presented above. For the advective-dispersive streamtube approach, a multimodal traveltime *pdf* is obtained with early peaks to characterize the peak of the integrated BTC and late peaks to characterize the breakthrough tail (Figure 3a). For the stochastic-convective model with mass transfer, spiky local BTCs are calculated because local dispersion is neglected, which may lead to a very spiky advective traveltime distribution. Here we adopt a small value of $\langle \varepsilon \rangle$ to avoid this computational shortcoming (Figure 3b). A smoother traveltime distribution is obtained because part of the

Table 4. Mixing Parameters as a Function of Temporal Moments of Local Breakthrough Curves

Model	Apparent Inverse Peclet Number, $\langle \varepsilon \rangle$	Apparent Capacity, $\langle \kappa \rangle$	Apparent Characteristic Timescale, $\langle \tau_{ad} \rangle$
Advective-dispersive streamtube approach	0.229	0	0
Stochastic-convective transport with mass transfer	0.001	1.778	$8.077 \times 10^5 s$
Advective-dispersive streamtube with mass transfer	0.0758	1	$6.667 \times 10^5 s$

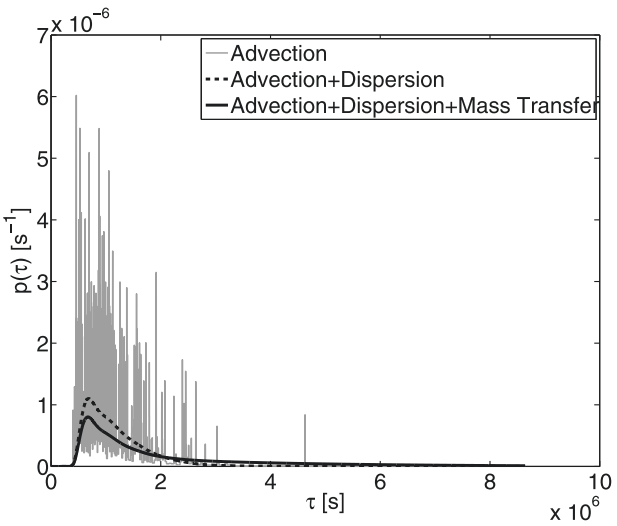

Figure 3. Numerical results of traveltimes simulated by the spatial transport model for the cases: advection alone, advection and local dispersion, and advection, local dispersion, and mass transfer.

dispersion effects are included in the traveltime distribution. Figure 3c shows the advective traveltime distribution for the advective-dispersive streamtube model with mass transfer, which is multimodal with earlier peaks than Figure 3a because the breakthrough tail is described by mass transfer. Because the model predicts fairly smooth local BTCs, the traveltime distribution does not need to be smooth in order to meet the integrated BTC. The non-negativity constraint leads to a multimodal traveltime *pdf*.

[58] Figure 5 shows the fits of the integrated BTC. Particularly, satisfactory fitting of the BTC tail is obtained within the current timeframe of 100 days. For the advective-dispersive streamtube approach, a later peak of the traveltime *pdf* is needed to characterize the tailing of the integrated BTC, while the other two models describe the tailing by mass transfer. This result demonstrates that there is freedom for the combinations of mixing parameters and traveltime *pdf* s to fit the BTC and describe the tailing.

7.3. Reactive Transport

[59] The results of conservative tracers cannot be used to justify which traveltime model is better in approximating the transport process because all of them can reproduce the integrated BTC. To examine the performance of traveltime-based models, we consider reactive transport of compounds undergoing a dual Michaelis-Menten problem with 1:1:1 stoichiometry:

$$\mathrm{A} + \mathrm{B} \rightarrow \mathrm{C}$$

The hydraulic conductivity field and the transport parameters are the same as those presented in the previous section. We assume the domain is initially filled with compound B at concentration one. A solution of compound A with concentration one is continuously injected at the inflow boundary. The transport parameters for all compounds are identical. The reaction rates of the dual Michaelis-Menten problem are given by:

$$r_m^{(A)} = r_m^{(B)} = \quad r_m^{(C)} = \quad r_{\max} \frac{c_m^{(A)}}{K_A + c_m^{(A)}} \times \frac{c_m^{(B)}}{K_B + c_m^{(B)}} \tag{48}$$

in which $r_m^{(A)}$, $r_m^{(B)}$, and $r_m^{(C)}$ are the reaction rates of species A, B, and C, respectively; $c_m^{(A)}$, $c_m^{(B)}$, and $c_m^{(C)}$ are mobile-phase concentrations; $r_{\max}$ is the maximum reaction rate; and K_A and K_B are the half saturation coefficients. The reaction rates in the immobile phase are considered zero. Equation (48) is often employed to describe bioreactive transport in the mobile phase under non-growth conditions. The reaction parameters are chosen as: $K_A = K_B = 0.1 \times c_0$, and $r_{\max} = 1$/day, in which c_0 is the unit initial and injection concentration, respectively.

[60] Figure 6 compares the simulation results of the integrated BTCs of the reactive species A and B, and the product C at the outflow boundary simulated by the 2-D spatial transport model and the three traveltime-based mod-

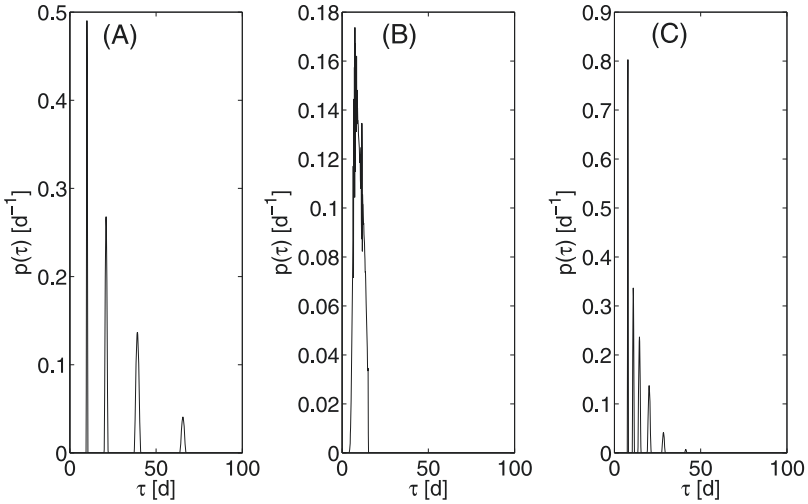

Figure 4. Advective traveltime *pdf*s estimated by the traveltime-based models. (a) Advective-dispersive model. (b) Stochastic-convective model with mass transfer. (c) Advective-dispersive model with mass transfer.

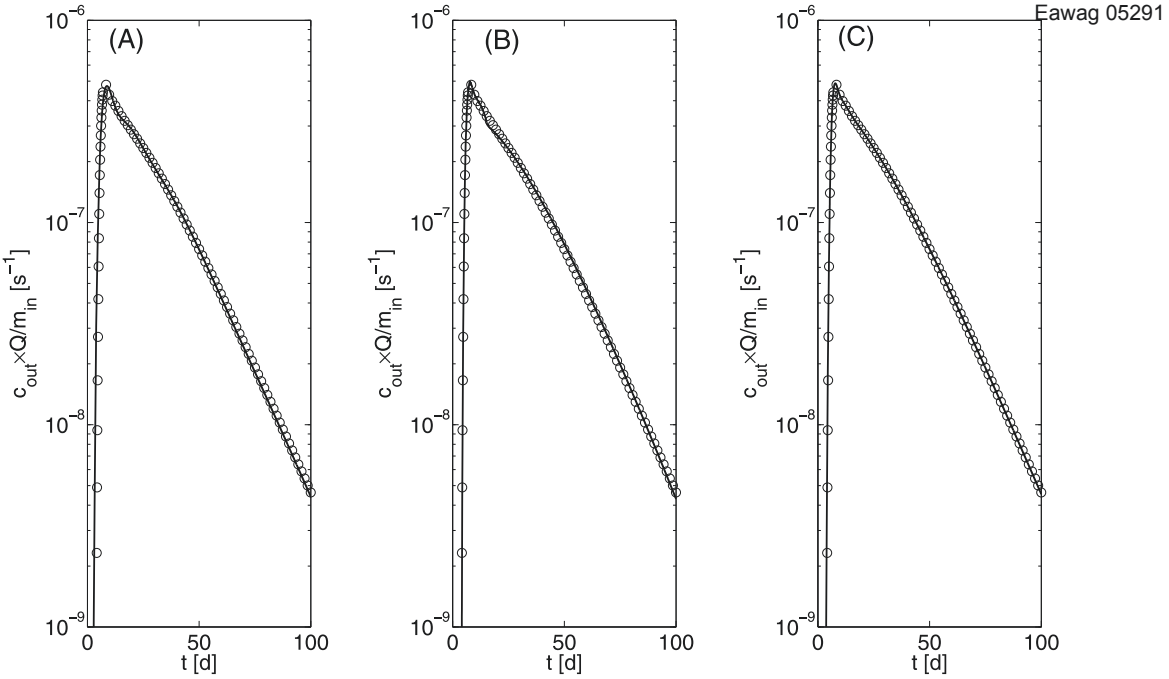

Figure 5. Fit of the integrated BTC by traveltime-based models (solid lines) in comparison to spatially explicit 2D simulation (circles). (a) Advective-dispersive model. (b) Stochastic-convective model with mass transfer. (c) Advective-dispersive model with mass transfer.

els based on the local and integrated conservative-tracer BTCs analyzed above. The results of the stochastic-convective model are not plotted because it neglects all mixing which would result in forming no product whatsoever. The advective-dispersive streamtube model gives the worst prediction of the BTC. Both the advective-dispersive model with and without mass transfer underpredict the mass of the reaction product. The best prediction is given by the

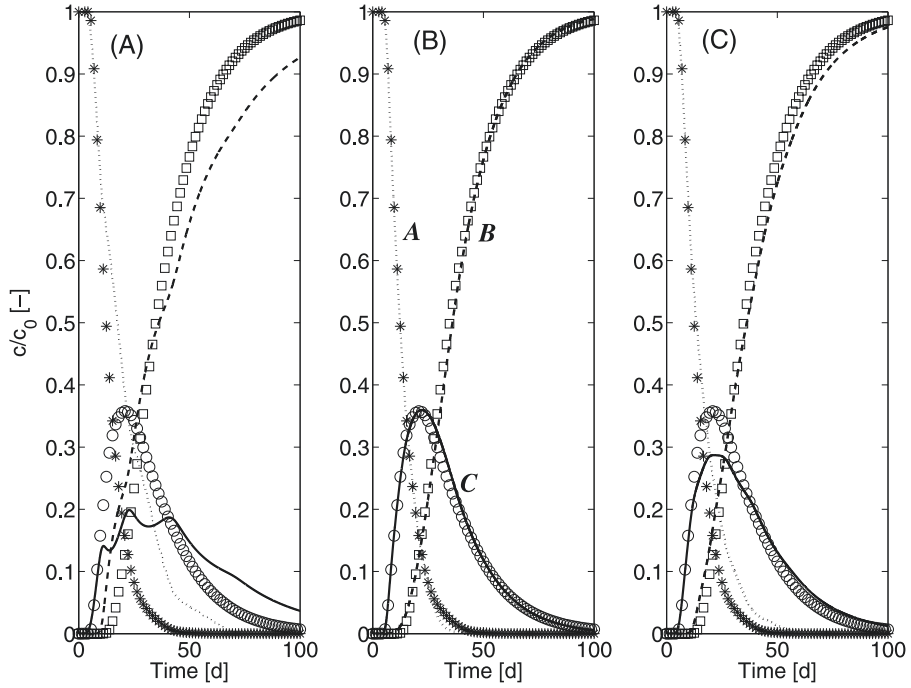

Figure 6. Integrated BTCs of the reactive species A and B and the reaction product C at the outflow boundary simulated by traveltime-based models using dual Michaelis-Menten kinetics. Symbols are numerical results from 2D simulations, and lines are results predicted by the traveltime-based models. (a) Advective-dispersive model. (b) Stochastic-convective model with mass transfer. (c) Advective-dispersive model with mass transfer.

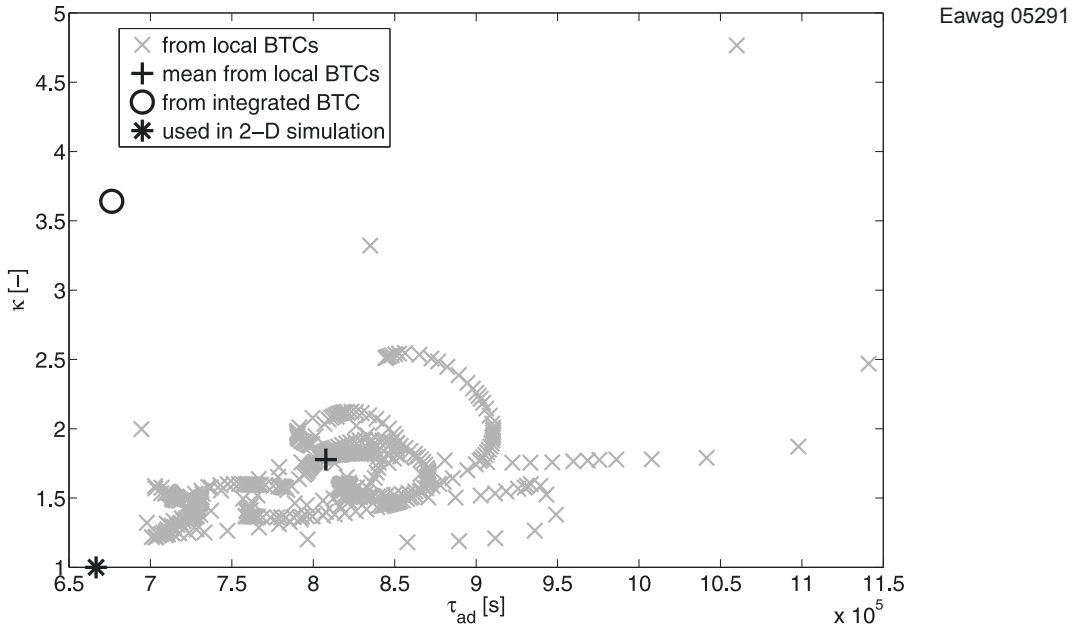

Figure 7. Apparent parameters, expressing mixing by mass transfer processes, as determined from temporal moments of the conservative tracer in the outflow. Crosses: estimated from local BTCs; plus: mean of parameters estimated from local BTCs; circle: estimated from integrated BTC; asterisk: true local values used in the 2D simulation.

stochastic-convective model with apparent mass transfer. This is the only model in which kinetic mass transfer coefficients are estimated from local BTCs; in all other models these coefficients are either set to zero or to the true local values. This implies, that approximating the effects of mixing introduced by transverse dispersion in a traveltime-based model is better done by using apparent kinetic mass transfer rather than apparent longitudinal dispersion coefficients. The result is different from that presented by *Cirpka and Kitanidis* [2000b], in which mixing mechanisms considered in theoretical analyses and numerical studies include only longitudinal and transverse dispersion, but no mass transfer between mobile and immobile water. The test case in the study by *Cirpka and Kitanidis* [2000b] was based on multidimensional advective-dispersive transport in a mildly heterogeneous medium. In that case, the advective-dispersive streamtube approach worked very well. The present research shows that in the presence of such mass transfer, the advective-dispersive streamtube method (in which mixing is parameterized by intra-streamtube dispersion only) may not be appropriate for simulating mixing-controlled reactive transport. If intraparticle diffusion has to be added, or if the system is so heterogeneous that a parameterization by assuming stagnant water zones becomes appropriate, the advective-dispersive streamtube model is too restrictive in the range of possible shapes of local BTCs. Thus, to obtain more skewed local BTCs streamtube transport beyond advection and dispersion is needed. In addition, *Cirpka and Kitanidis* [2000b] used a parametric function in the estimation of the traveltime distribution, implying that the actual shape of the flux-averaged BTC is not fully exploited. However, both studies share the same characteristics, that is, the models with mixing parameters that are all estimated from local BTCs give the best simulation results.

7.4. Uncertainty Analysis

[61] The approach outlined above involves several steps subject to uncertainty. Conceptual uncertainty arises from the choice of parameterizing mixing. This has been demonstrated in the previous section. Parametric uncertainty is caused by (1) determining the mixing-related coefficients ε, κ and τ_{ad} from local BTCs of a conservative tracer and (2) evaluating the advective traveltime distribution $p(\tau)$ for given mixing coefficients. In the context of deconvolution, *Cirpka et al.* [2007] addressed the latter uncertainty by generating conditional realizations of traveltime distributions. Interestingly, the associated uncertainty bounds were comparably narrow. We conjecture that in practical applications the most critical point with respect to parametric uncertainty in our traveltime approaches lies in estimating the mixing-related coefficients. This is so, because these coefficients are estimated from a local breakthrough curves, which typically are available only in small numbers. Thus, if the few local BTCs available are not representative in their mixing characteristics the entire prediction of reactive transport integrated over the control plane is erroneous.

[62] In our numerical example, we have access to 500 local BTCs of a conservative tracer, and we have used mixing-related coefficients averaged over all local BTCs in the analyses above. Figure 7 shows the apparent mass transfer parameters, κ and τ_{ad}, determined from the temporal moments of all local BTCs using the stochastic-convective model with mass transfer. Figure 7 also includes the erroneous parameters that were determined from the integrated BTC. The set of local values gives us the opportunity of quantifying the uncertainty in predicting macroscopic reactive transport caused by the choice of the local observation points, at which the mixing-related coefficients are estimated from local BTCs of the conservative tracer.

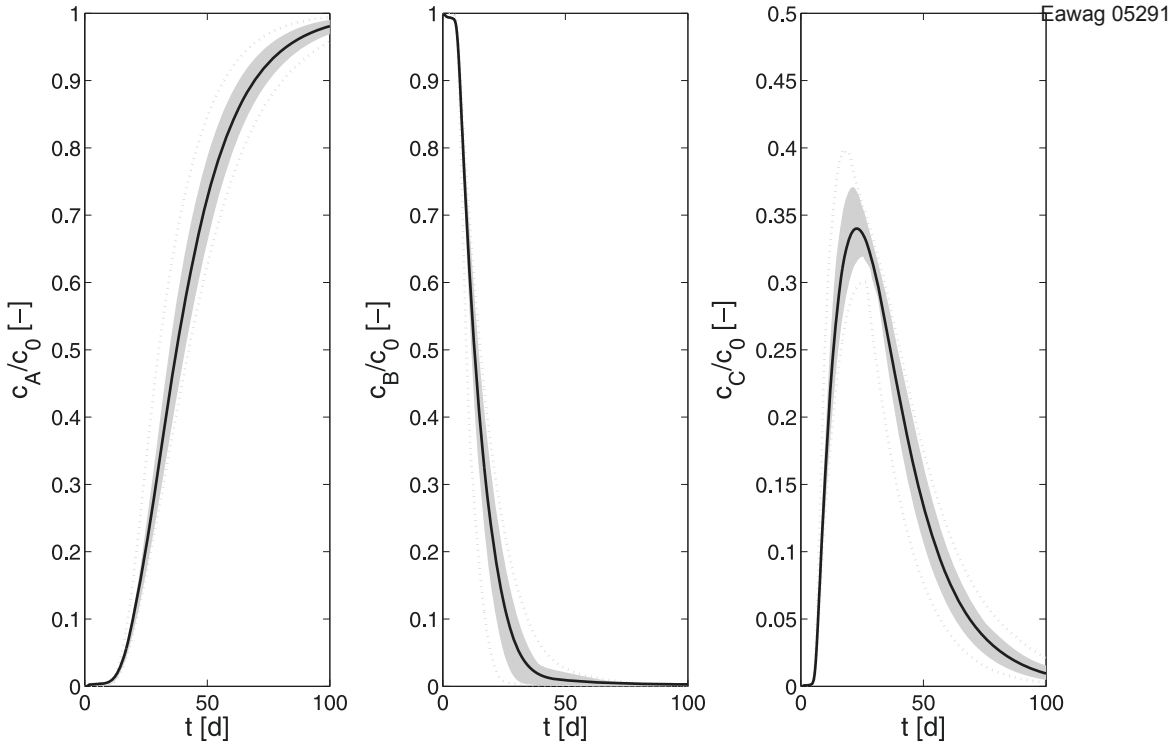

Figure 8. Statistical bounds of integrated BTCs of the reactive species A and B and the reaction product C. Solid lines: mean BTCs; gray band: 16 to 84 percentiles; dotted lines: 95% confidence interval.

[63] For each pair of locally determined κ- and τ_{ad}-values, we go through the procedure outlined above. That is, we obtain 500 advective-traveltime distributions $p(\tau)$, each associated to a particular set of κ- and τ_{ad}-values. For each of these 500 parameter sets, we compute the integrated BTCs of the reactive compounds in the outflow according to equation (47). Finally, for each time t we arrive at 500 different predictions of the reactive-species concentrations $C_A(t)$, $C_B(t)$, and $C_C(t)$, averaged over the control plane. This brute-force sampling procedure guarantees that the uncertainty of reactive-species concentrations, caused by choosing particular local observation points of the conservative tracer, is adequately described by the full statistical distributions of $C_A(t)$, $C_B(t)$, and $C_C(t)$. Figure 8 presents metrics of these statistical distributions. The black lines are the mean reactive-species BTCs predicted from the ensemble of 500 parameter sets. The gray bands denote the 16 to 84 percentiles, which would correspond to ± one standard deviation, if the distributions were Gaussian, whereas the dotted lines represent the 2.5 to 97.5 percentiles, covering the 95% confidence interval. Figure 8 indicates that the uncertainty introduced by choosing only a few local BTCs of the conservative tracer for the assessment of mixing-related parameters is not too big, at least not in the given example. Of course, as indicated in Figure 7, a few outliers of apparent mass transfer coefficients determined from local conservative-tracer BTCs exist. However, these points are outside the 95% confidence interval.

8. Conclusions

[64] The advantages of traveltime-based models for describing transport-controlled reactive mixing include (1) no thorough characterizations of aquifer heterogeneities and transport mechanisms are required; (2) computation efforts are minimized by transforming three-dimensional problems in spatial coordinates to one-dimensional problems in the traveltime domain; (3) mixing and spreading may be distinguished by transport models and advective traveltime distributions; and (4) traveltime distributions may be conveniently updated by tracer tests for simulating long-term groundwater remediation transport cases. Traveltime-based reactive transport models are well suited to predict reactive species concentrations at points where conservative tracer BTCs are available, that is, traveltime distributions can be conveniently evaluated. In order to make reactive transport predictions at locations where conservative tracer concentrations are not available, either conservative tracer test data should be collected at these locations or spatial data needs to be incorporated to evaluate the spatial distribution of traveltimes [e.g., *Crane and Blunt*, 1999; *Cirpka and Kitanidis*, 2001].

[65] Two key issues are associated with traveltime-based models. One is the description of mixing, and the other is the estimation of traveltime distribution. Longitudinal dispersion and kinetic mass transfer can be incorporated into traveltime-based models to characterize mixing. However, unlike the spatial models in which parameters for dispersion and kinetic mass transfer can be interpreted as the true values, traveltime-based models use fictitious or apparent parameters because (1) transverse dispersion cannot be explicitly described and (2) traveltime is unidirectional, whereas the actual traveling path is three-dimensional. A determined traveltime distribution holds only for the mixing description used in the determination procedure. In heter-

ogenous fields, traveltime distributions are likely to be multimodal curves with long tails. It may be challenging to describe these curves by parametric distributions. Such limitations can be overcome by nonparametric approaches allowing traveltime distributions to adapt freely to the needs of the problem.

[66] Both local and integrated BTCs are required to establish a traveltime-based model. We propose to use the local BTCs to estimate the mixing parameters, and then apply the nonparametric approach to estimate the corresponding traveltime distribution. However, conservative tracer BTCs only may not be sufficient to determine which traveltime-based model is more appropriate for reactive-transport simulations because the nonparametric approach allows good fitting of the integrated BTC for variable mixing models, e.g., there is freedom for the combinations of mixing parameters and traveltime *pdf* s to fit conservative BTCs. The reactive-transport case conducted in this research indicates that the mixing introduced by local dispersion and mass transfer, which is neglected by original traveltime-based models, are best described by the apparent mean mass transfer, and may not be described as well by apparent longitudinal dispersion.

References

Bellin, A., and Y. Rubin (2004), On the use of peak concentration arrival times for the inference of hydrogeological parameters, *Water Resour. Res.*, *40*, W07401, doi:10.1029/2003WR002179.

Bellin, A., R. Rubin, and A. Rinaldo (1994), Eulerian-Lagrangian approach for modeling of flow and transport in heterogeneous geological formations, *Water Resour. Res.*, *30*, 2913 2924.

Berkowitz, B., A. Cortis, M. Dentz, and H. Scher (2006), Modeling non-Fickian transport in geological formations as a continuous time random walk, *Rev. Geophys.*, *44*, RG2003, doi:10.1029/2005RG000178.

Berkowitz, B., and H. Scher (1997), Anomalous transport in random fracture networks, *Phys. Rev. Lett.*, *79*, 4038 4041.

Berkowitz, B., and H. Scher (1998), Theory of anomalous chemical transport in random fracture networks, *Phys. Rev. E*, *57*, 5858 5869.

Berkowitz, B., H. Scher, and S. E. Silliman (2000), Anomalous transport in laboratory-scale, heterogeneous porous media, *Water Resour. Res.*, *36*, 149 158.

Brusseau, M. L. (1992), Transport of rate-limited sorbing solutes in heterogeneous porous-media Application of a one-dimensional multifactor nonideality model to field data, *Water Resour. Res.*, *28*, 2485 2497.

Chen, W. L., and R. J. Wagenet (1995), Solute transport in porous-media with sorption-site heterogeneity, *Environ. Sci. Technol.*, *29*, 2725 2734.

Cirpka, O. A. (2002), Choice of dispersion coefficients in reactive transport calculations on smoothed fields, *J. Contam. Hydrol.*, *58*, 261 282.

Cirpka, O. A. (2005), Effects of sorption on transverse mixing in transient flows, *J. Contam. Hydrol.*, *78*, 207 229.

Cirpka, O. A., M. N. Fienen, M. Hofer, E. Hoehn, A. Tessarini, R. Kipfer, and P. K. Kitanidis (2007), Analyzing bank filtration by deconvoluting times series of electric conductivity, *Ground Water*, *45*(3), 318 328.

Cirpka, O. A., E. O. Frind, and R. Helmig (1999a), Numerical methods for reactive transport on rectangular and streamline-oriented grids, *Adv. Water Resour.*, *22*, 711 728.

Cirpka, O. A., E. O. Frind, and R. Helmig (1999b), Numerical simulation of biodegradation controlled by transverse mixing, *J. Contam. Hydrol.*, *40*, 159 182.

Cirpka, O. A., E. O. Frind, and R. Helmig (1999c), Streamline-oriented grid-generation for transport modelling in two-dimensional domains including wells, *Adv. Water Resour.*, *22*, 697 710.

Cirpka, O. A., and P. K. Kitanidis (2000a), An advective-dispersive streamtube approach for the transfer of conservative tracer data to reactive transport, *Water Resour. Res.*, *36*, 1209 1220.

Cirpka, O. A., and P. K. Kitanidis (2000b), Characterization of mixing and dilution in heterogeneous aquifers by means of local temporal moments, *Water Resour. Res.*, *36*, 1221 1236.

Cirpka, O. A., and P. K. Kitanidis (2001), Traveltime based model of bioremediation using circulation wells, *Ground Water*, *39*, 422 432.

Coats, K. H., and B. D. Smith (1964), Dead-end pore volume and dispersion in porous media, *Soc. Pet. Eng. J.*, *4*, 73 81.

Crane, M. J., and M. J. Blunt (1999), Streamline-based simulation of solute transport, *Water Resour. Res.*, *35*, 3061 3078.

Cunningham, J., and P. V. Roberts (1998), Use of temporal moments to investigate the effects of nonuniform grain-size distribution on the transport of sorbing solutes, *Water Resour. Res.*, *34*, 1415 1425.

Cvetkovic, V. D., and D. Dagan (1994), Transport of kinetically sorbing solute by steady random velocity in heterogeneous porous formations, *J. Fluid Mech.*, *265*, 189 215.

Cvetkovic, V. D., G. Dagan, and H. Cheng (1998), Contaminant transport in aquifers with spatially variable hydraulic and sorption properties, *Proc. R. Soc. London, Ser. A*, *454*, 2173 2207.

Cvetkovic, V. D., and R. Haggerty (2002), Transport with multiple-rate exchange in disordered media, *Phys. Rev. E*, *65*, 051308.

Dagan, G. (1989), *Flow and Transport in Porous Formations*, Springer-Verlag, New York.

Datta-Gupta, A., S. Yoon, D. W. Vasco, and G. A. Pope (2002), Inverse modeling of partitioning interwell tracer tests: A streamline approach, *Water Resour. Res.*, *38*(6), 1079, doi:10.1029/2001WR000597.

Dentz, M., and B. Berkowitz (2003), Transport behavior of a passive solute in continuous time random walks and multirate mass transfer, *Water Resour. Res.*, *39*(5), 1111, doi:10.1029/2001WR000163.

Dentz, M., H. Kinzelbach, S. Attinger, and W. Kinzelbach (2000), Temporal behavior of a solute cloud in a heterogeneous porous medium. 1: Point-like injection, *Water Resour. Res.*, *36*, 3591 3604.

Di Donato, G., and M. J. Blunt (2004), Streamline-based dual-porosity simulation of reactive transport and flow in fractured reservoirs, *Water Resour. Res.*, *40*, W04203, doi:10.1029/2003WR002772.

Di Donato, G., E. O. Obi, and M. J. Blunt (2003), Anomalous transport in heterogeneous media demonstrated by streamline-based simulation, *Geophys. Res. Lett.*, *30*(12), 1608, doi:10.1029/2003GL017196.

Dykaar, B. B., and P. K. Kitanidis (1992), Determination of the effective hydraulic conductivity for heterogeneous porous media using a numerical spectral approach. 1: Method, *Water Resour. Res.*, *28*, 1155 1166.

Fiori, A., I. Jankovic, and G. Dagan (2006), Modeling flow and transport in highly heterogeneous three-dimensional aquifers: Ergodicity, Gaussianity, and anomalous behavior. 2: Approximate semianalytical solution, *Water Resour. Res.*, *42*, W06D13, doi:10.1029/2005WR004752.

Fiori, A., and G. Dagan (2000), Concentration fluctuations in aquifer transport: A rigorous first-order solution and applications, *J. Contam. Hydrol.*, *45*, 139 162.

Gelhar, L. W. (1993), *Stochastic Subsurface Hydrology*, Prentice-Hall Inc., Englewood Cliffs, N. J.

Ginn, T. R. (2001), Stochastic-convective transport with nonlinear reactions and mixing: Finite streamtube ensemble formulation for multicomponent reaction systems with intra-streamtube dispersion, *J. Contam. Hydrol.*, *47*, 1 28.

Ginn, T. R., E. M. Murphy, A. Chilakapati, and U. Seeboonruang (2001), Stochastic-convective transport with nonlinear reaction and mixing: Application to intermediate-scale experiments in aerobic biodegradation in saturated porous media, *J. Contam. Hydrol.*, *48*, 121 149.

Ginn, T. R., C. S. Simmons, and B. D. Wood (1995), Stochastic-convective transport with nonlinear reaction: Biodegradation with microbial growth, *Water Resour. Res.*, *31*, 2689 2700.

Gramling, C. M., C. F. Harvey, and L. C. Meigs (2002), Reactive transport in porous media: A comparison of model prediction with laboratory visualization, *Environ. Sci. Technol.*, *36*, 2508 2514.

Haggerty, R., and S. M. Gorelick (1995), Multiple-rate mass transfer for modeling diffusion and surface reactions in media with pore-scale heterogeneity, *Water Resour. Res.*, *31*, 2383 2400.

Haggerty, R., and S. M. Gorelick (1998), Modeling mass transfer processes in soil columns with pore-scale heterogeneity, *Soil Sci. Soc. Am. J.*, *62*, 62 74.

Hassan, A. E., R. Andricevic, and V. D. Cvetkovic (2001), Computational issues in the determination of solute discharge moments and implications or comparison to analytical solutions, *Adv. Water Resour.*, *24*, 617 619.

Janssen, G., O. A. Cirpka, and S. E. A. T. M. van der Zee (2006), Stochastic analysis of nonlinear biodegradation in regimes controlled by both chromatographic and dispersive mixing, *Water Resour. Res.*, *42*, W01417, doi:10.1029/2005WR004042.

Kapoor, V., L. W. Gelhar, and F. Miralles-Willem (1997), Bimolecular second-order reactions in spatially varying flows: Segregation induced scale-dependent transformation rates, *Water Resour. Res.*, *33*, 527 536.

Kitanidis, P. K. (1988), Prediction by the method of moments of transport in a heterogeneous formation, *J. Hydrol.*, *102*, 453 473.

Kitanidis, P. K. (1994), The concept of the dilution index, *Water Resour. Res.*, *30*, 2011 2026.

Kreft, A., and A. Zuber (1978), On the physical meaning of the dispersion equation and its solutions for different initial and boundary conditions, *Chem. Eng. Sci.*, *33*, 1471 1480.

Lawrence, A., X. Scanchez-Vila, and Y. Rubin (2002), Conditional moments of the breakthrough curves of kinetically sorbing solutes in heterogeneous porous media using multi-rate mass transfer models for sorption and desorption, *Water Resour. Res.*, *38*(1), 1248, doi:10.1029/2001WR001006.

Lee, L. S., P. S. C. Rao, M. L. Brusseau, and R. A. Ogwada (1988), Nonequilibrium sorption of organic contaminants during flow through columns of aquifer materials, *Environ. Toxic Chem.*, *7*, 779 793.

Loaiciga, H. A. (2004), Residence time, groundwater age, and solute output in steady-state groundwater systems, *Adv. Water Resour.*, *27*, 681 688.

Luo, J., O. A. Cirpka, M. N. Fienen, W.-M. Wu, T. L. Mehlhorn, J. Carley, P. M. Jardine, C. S. Criddle, and P. K. Kitanidis (2006), A parametric transfer function methodology for analyzing reactive transport in nonuniform flow, *J. Contam. Hydrol.*, *83*, 27 41.

Luo, J., W.-M. Wu, J. Carley, C. Ruan, B. Gu, P. M. Jardine, C. S. Criddle, and P. K. Kitanidis (2007), Hydraulic performance analysis of a multiple injection-extraction well system, *J. Hydrol.*, *336*, 294 302.

Margolin, G., M. Dentz, and B. Berkowitz (2003), Continuous time random walk and multirate mass transfer modeling of sorption, *Chem. Phys.*, *295*, 71 80.

Michalak, A. M., and P. K. Kitanidis (2000), Macroscopic behavior and random-walk particle tracking of kinetically sorbing solutes, *Water Resour. Res.*, *36*, 2133 2146.

Miralles-Wilhelm, F., L. W. Gelhar, and V. Kapoor (1997), Stochastic analysis of oxygen-limited biodegradation in three-dimensionally heterogeneous aquifers, *Water Resour. Res.*, *33*, 1251 1263.

Molz, F. J., and M. A. Widdowson (1988), Internal inconsistencies in dispersion-dominated models that incorporate chemical and microbial kinetics, *Water Resour. Res.*, *24*, 615 619.

Nauman, E. B., and B. A. Buffham (1983), Mixing in continuous flow systems, John Wiley, New York.

Obi, E. O., and M. J. Blunt (2004), Streamline-based simulation of advective-dispersive solute transport, *Adv. Water Resour.*, *27*, 913 924.

Oya, S., and A. J. Valocchi (1998), Transport and biodegradation of solutes in stratified aquifers under enhanced in situ bioremediation conditions, *Water Resour. Res.*, *34*, 3323 3334.

Press, W. H., S. A. Teukolsky, W. T. Vetterling, and B. P. Flannery (1992), *Numerical Recipes in FORTRAN 77: The Art of Scientific Computation*, Cambridge Univ. Press, New York.

Quinodoz, H., and A. J. Valocchi (1993), Stochastic-analysis of the transport of kinetically sorbing solutes in aquifers with randomly heterogeneous hydraulic conductivity, *Water Resour. Res.*, *29*, 3227 3240.

Raje, D. S., and V. Kapoor (2000), Experimental study of bimolecular reaction kinetics in porous media, *Environ. Sci. Technol.*, *34*, 1234 1239.

Robinson, B. A., and H. S. Viswanathan (2003), Application of the theory of micromixing to groundwater reactive transport models, *Water Resour. Res.*, *39*(11), 1313, doi:10.1029/2003WR002368.

Rubin, Y. (2003), *Applied Stochastic Hydrogeology*, Oxford Univ. Press, Inc., New York.

Rubin, Y., M. A. Cushey, and A. Wilson (1997), The moments of the breakthrough curves of instantaneously and kinetically sorbing solutes in heterogeneous geologic media: Predication and parameter inference from field measurements, *Water Resour. Res.*, *33*, 2465 2481.

Rubin, Y., and G. Dagan (1992), Conditional estimation of solute travel time in heterogenous formations: Impact of transmissivity measurements, *Water Resour. Res.*, *25*, 1033 1040.

Rubin, Y., and S. Ezzedine (1997), The travel times of solutes at the Cape Cod tracer experiment: Data analysis, and structural parameter inference: Theory and unconditional numerical simulations, *Water Resour. Res.*, *33*, 1537 1547.

Sardin, M., D. Schweich, F. J. Leij, and M. T. van Genuchten (1991), Modeling the nonequilibrium transport of linearly interacting solutes in porous media: A review, *Water Resour. Res.*, *27*, 2287 2307.

Selroos, J. O. (1995), Temporal moments for nonergodic solute transport in heterogeneous aquifers, *Water Resour. Res.*, *31*, 1705 1712.

Selroos, J. O., and V. Cvetkovic (1992), Modeling solute advection coupled with sorption kinetics in heterogenous formations, *Water Resour. Res.*, *28*, 1271 1278.

Semprini, L., and P. L. McCarty (1991), Comparison between model simulation on field results for in-situ biorestoration of chlorinated aliphatics. Part 1: Biostimulation of the methanotrophic bacteria, *Ground Water*, *29*, 365 374.

Shapiro, A. M., and V. D. Cvetkovic (1988), Stochastic-analysis of solute arrival time in heterogeneous porous-media, *Water Resour. Res.*, *24*, 1711 1718.

Shapiro, A. M., and V. D. Cvetkovic (1990), Mass arrival of sorptive solute in heterogeneous porous-media, *Water Resour. Res.*, *26*, 2057 2067.

Simic, E., and G. Destouni (1999), Water and solute residence times in a catchment: Stochastic-mechanistic model interpretation of 18O transport, *Water Resour. Res.*, *35*, 2109 2119.

Simmons, C. S. (1982), A stochastic-convective transport representation of dispersion in one-dimensional porous-media systems, *Water Resour. Res.*, *18*, 1193 1214.

Simmons, C. S., T. Ginn, and B. Wood (1995), Stochastic-convective transport with nonlinear reaction: Mathematical framework, *Water Resour. Res.*, *31*, 2675 2688.

Sturman, P. J., P. S. Stewart, A. B. Cunningham, E. J. Bouwer, and J. H. Wolfram (1995), Engineering scale-up of in situ bioremediation processes: A review, *J. Contam. Hydrol.*, *19*, 171 203.

Valocchi, A. J. (1989), Spatial moment analysis of the transport of kinetically adsorbing solutes through stratified aquifers, *Water Resour. Res.*, *25*, 273 279.

van der Zee, S. E. A. T. M., and W. H. van Riemsdijk (1987), Transport of reactive solutes in spatially variable soil systems, *Water Resour. Res.*, *23*, 2059 2069.

Villermaux, J. (1987), Chemical-engineering approach to dynamic modeling of linear chromatography A flexible method for representing complex phenomena from simple concepts, *J. Chromatogr.*, *406*, 11 26.

Vogel, C. R. (2002), *Computational Methods for Inverse Problems*, Society for Industrial and Applied Mathematics (SIAM), Philadelphia, Pa.

Weeks, S. W., and G. Sposito (1998), Mixing and stretching efficiency in steady and unsteady groundwater flows, *Water Resour. Res.*, *34*, 3315 3322.

Woodbury, A. D., and Y. Rubin (2000), A full-Bayesian approach to parameter inference from tracer travel time moments and investigation of scale effects at the Cape Cod experimental site, *Water Resour. Res.*, *36*, 159 171.

O. A. Cirpka, Swiss Federal Institute of Aquatic Science and Technology (Eawag), Überlandstr. 133, 8600 Dübendorf, Switzerland.

J. Luo, School of Civil and Environmental Engineering, Georgia Institute of Technology, Atlanta, GA 30332-0355, USA. (jianluo@ce.gatech.edu)